ARTICLE

Mangrove extent mapping using different mangrove vegetation indices and sentinel-2 for ecosystem accounting in Occidental Mindoro, Philippines

Adrian Pablo V. Sasi*[1], Cristino L. Tiburan Jr.[1,4], Gem B. Castillo[2], Canesio D. Predo[1,4], Asa Jose U. Sajise[3,4], Juan M. Pulhin[4,5], Arnan B. Araza[6], Catherine S. Anders[4], Rosario V. Tatlonghari[4,7], Dannica Rose G. Aquino[4], Grace Anne S. Malolos[4], Karen M. Pajadan[4], Christian Ray C. Buendia[4], and Pauline Cielo P. Palma[4]

[1]Institute of Renewable Natural Resources, College of Forestry and Natural Resources, UPLB, Laguna, Philippines
[2]Resources, Environment and Economics Center for Studies, Inc., Philippines
[3]Department of Economics, College of Economics and Management, UPLB, Laguna, Philippines
[4]UPLB Interdisciplinary Studies Center for Integrated Natural Resources and Environment Management, UPLB, Laguna
[5]Department of Social Forestry and Forest Governance, College of Forestry and Natural Resources, UPLB, Laguna, Philippines
[6]Wageningen University & Research
[7]College of Development Communication, UPLB, Laguna, Philippines

ABSTRACT

The he Philippines is home to about half of the world's 65 mangrove species, representing 50% of mangroves globally. As an archipelagic country, mangrove forests offer a variety of ecosystem goods and services, from coastal protection to carbon sequestration, which play a vital role in climate change mitigation. Understanding mangroves' changing extent and condition is critical and valued, as these impact climate, biodiversity, and ecosystem service provision. However, little has been done to account for these attributes. Thus, the study aimed to construct physical ecosystem accounts for mangroves in Occidental Mindoro, Philippines, encompassing spatial distribution and extent, and develop a physical accounting table. Using cloud-based remote sensing on the Google Earth Engine (GEE) platform, this research contributes to broader ecosystem accounting efforts for the West Philippine Sea, providing evidence-based insights for effective policymaking and decision-making. Mangrove extent modeling was conducted using a three-tiered approach, guided by the spatial framework

*Corresponding author
Email Address: avsasi@up.edu.ph
Date received: 15 March 2024
Date revised: 12 March 2025
Date accepted: 24 June 2025
DOI: https://doi.org/10.54645/202518SupKKO-31

KEYWORDS

Mangrove extent mapping, Ecosystem accounts, Google Earth Engine, SEEA

of the System of Environmental-Economic Accounting (SEEA) Ecosystem Accounting, to improve accuracy.

Vegetation indices such as Mangrove Vegetation, Normalized Difference Vegetation, Normalized Difference Mangrove, Modified Normalized Difference Water, and the Green Chlorophyll Vegetation were employed. Statistical parameters for feature objects were selected and applied in the random forest classifier. In 2021-2023, during the dry season with lesser clouds, composite images were produced by combining spatially overlapping ones into a single picture based on an aggregation function. These indices delineated the area of mangroves using remotely sensed imagery efficiently and precisely. Combining these spectral indices resulted in an overall mangrove extent of about 2,096.74 ha, with an overall classification accuracy of 87.33 percent and a Kappa coefficient of 0.80. Similarly, Sentinel-2A images and the GEE platform accurately assessed changes in the extent of mangrove forests within the coastal ecosystems of the West Philippine Sea.

INTRODUCTION

The Philippines' unique geographical features have led to high terrestrial and marine endemism, making it one of the world's most biodiverse countries (Carpenter and Springer 2005). The country boasts a coastline stretching over 36,989 km, which is one of the longest in the world, and is home to diverse coastal and marine habitats (CIA 2007). Along these areas lie diverse mangrove ecosystems that are home to 65 mangrove species in the country (Kathiresan and Bingham 2001 as cited by Primavera et al. 2004), representing 50 percent of the global total (Primavera et al. 2004). This led to the Philippines being recognized as one of the 15 leading mangrove-rich countries worldwide (Long and Giri 2011). According to Brown and Fischer (1918), the extent of mangroves in the Philippines during the 1920s was estimated to be between 400,000 and 500,000 ha. However, by the year 2000, it had decreased by almost 50 percent. In the study of Garcia et al. (2014) on the status of Philippine mangroves, potential threats were driven by aquaculture development, land conversion to agricultural use, urbanization and an increase in human settlements, deforestation, and fuel and charcoal making

The Philippine government heavily supported aquaculture and shrimp farming in the 1970s (DENR, 2013). This was driven by good market prices and policies like PD 704 (Fisheries Decree of 1975), which offered loans and land use rights for fishpond construction (DENR, 2013). While the Forestry Code permitted some protection for mangroves, it failed to enforce these regulations, resulting in the conversion of large areas of mangroves into fishponds and a sharp decline in extent (DENR, 2013).

Several studies have identified aquaculture development as the most significant potential threat to the diversity of mangrove species, followed by urbanization, conversion to agriculture, overutilization for manufacturing uses such as timber and charcoal making, and climate change (Garcia et al. 2014). In response to the rapid decline of mangroves due to aquaculture in the 1970s, Philippine environmental policy in the 1980s shifted decisively towards conservation. Several key developments, including constitutional entrenchment, protected area designation, buffer zone management, and rehabilitation initiatives, marked this legislative transformation (DENR, 2013). Conservation trends emerged in the 1980s and persisted throughout the 1990s. In addition, the government implemented policies to oversee the management of mangroves, emphasizing the engagement of communities, Non-Government Organizations (NGOs), and People's Organizations (POs) (DENR, 2013).

Consequently, approximately 3 percent of the 7.2M ha of forest cover reported in 2003 is mangrove (FMB, 2003). According to the latest statistics from the National Mapping and Resource Information Authority (NAMRIA) on terrestrial land cover, the country comprises around 6.6M ha of forest, which encompasses closed, open, and mangrove (NAMRIA, 2020). The mangrove forest, which accounts for 4.68 percent of the total forest cover, or 311,512.54 ha, is mostly found in the island of Palawan, Bangsamoro Autonomous Region in Muslim Mindanao (BARMM), and Region 8, which have the highest distribution (NAMRIA, 2020).

Understanding mangroves' changing extent and condition is critical and valued, as these impact climate, biodiversity, and ecosystem service provision. Over the past decades, gains and losses in the extent of mangrove ecosystems have been observed. Given that these structurally complex ecosystems serve as crucial breeding grounds for fishes, minimize shoreline erosion, reduce the effects of flooding and waves, and maintain and regulate coastal elevation in the event of sea level rise, the loss of their extent can impair the flow of these services. In contrast, the gains in mangrove extent increase carbon accumulation and storage and floral and faunal biodiversity. Mangroves are important, and thorough monitoring is required to ensure their survival and optimize their contribution to the preservation of the marine and coastal environment. This emphasizes the importance of developing and improving tools for producing mangrove extent maps, as well as detecting significant changes in mangrove ecosystem distribution over time.

The distribution of mangroves and monitoring initiatives has become crucial due to a significant decrease in their extent in recent years (Mariano et al. 2022). Field inventory is a highly efficient method for monitoring these ecosystems. However, it can be labor-intensive due to the inaccessibility and obstructions present in their habitat, such as pneumatophores and prop roots (Tomppo et al. 2008). Remote sensing (RS) technology enabled the observation and mapping of large areas with higher accuracy, speed, and scope than conventional field measurement but with some limitations and gaps. Pillodar et al. (2023) noted that the country's archipelagic features complicate mangrove RS mapping due to the need to evaluate numerous areas, the high cost of obtaining high-resolution datasets, and the software's limited applicability for mapping large areas. This suggests that an increasing number of papers were published using low- to medium-resolution data, and the overlapping canopies complicates species identification on the map.

In recent years, state-of-the-art technology in RS and Geographic Information Systems (GIS) has been rapidly developing, allowing more accurate information concerning its extent. Earth Observation data, such as Sentinel-2A, offers high-resolution optical imagery equipped with specialized bands useful for analyzing agricultural practices, forest management, and the assessment of land use and land cover dynamics (Chrysafis et al. 2020). Researchers are evaluating various approaches using Sentinel 2 data, including land use/land cover (LULC) mapping and change analysis (Baloloy 2021; Addabbo et al. 2016; Topaloğlu et al. 2017), vegetation change detection (Baloloy 2021; Eklundh et al. 2012), vegetation health assessment (Baloloy 2021; Rao et al. 2017), and species detection and recognition (Baloloy 2021; Immitzer et al. 2016). Sentinel 2 plays a significant role in mapping mangrove extent, enabling various categorization approaches like supervised, unsupervised, object-based, or index-based methods. Furthermore, it is capable of effectively mapping biophysical variables such as land use-land cover change detection, chlorophyll content, water content, and leaf area index (Drusch et al. 2012). Therefore, it performed coastal and inland water surveillance and assisted with risk assessment and in disaster mapping. Researchers have examined the effectiveness of various classification algorithms, including MLC (Maximum Likelihood Classification), SVM (Support Vector Machine), ANN (Artificial Neural Network), and RF (Random Forest), in mapping the extent of mangroves using Sentinel-2A satellite images. Each algorithm yielded varying accuracy levels, displaying promising results on mangrove extent mapping (Roslani et al. 2003; Giri and Muhlhausen 2008; Deilmai et al. 2014; Kanniah et al. 2015; Ma et al. 2017; Liu et al. 2021, as cited by Baloloy 2021).

In this study, the functions of GEE and Sentinel-2A to produce a map extent of Occidental Mindoro for ecosystem accounting were used. GEE is a platform that maintains satellite imagery in a publicly accessible data archive, as it provides cloud-based environmental data analytics (Gorelick et al. 2017). This collection contains historical images of the Earth that span over 40 years. Sentinel-2A satellite imagery, processed through the GEE Cloud Computing platform, will be used in this study to evaluate its effectiveness for mangrove mapping in the coastal areas of Occidental Mindoro.

The extent of Occidental Mindoro's mangrove ecosystem is currently available in global datasets such as Global Mangrove Watch and IUCN Global Ecosystem Typology 2.0 as well as local datasets developed by NAMRIA through land cover and coastal resources maps. Other sources of ecosystem extent on mangroves are available in Environmental Systems Research Institute (ESRI) Land Cover Time Series (Karra et al. 2021), Mangrove Vegetation Index-based Mangrove Map (Baloloy et al. 2020), National Aeronautics and Space Administration – Jet Propulsion Laboratory (NASA-JPL) Global Mangrove Map (Giri et al. 2011 and Simard et al. 2019), Climate Change Initiative Land Cover (ESA Climate Change Initiative 2017), European Space Agency (ESA) World Cover (Defourny et al. 2012), High-resolution Global Mangrove Forest (Jia et al. 2023), Dynamic World Data (Brown et al. 2022), and Global Land Cover Dataset (GLCFCS30D) (Li et al. 2023).

Hence, this research aimed to develop physical ecosystem accounts for mangroves in Occidental Mindoro aligned with the United Nations' System of Environmental Economic Accounting (SEEA) framework. Specifically, the study sought to: (1) map mangrove spatial distribution and quantify areal extent in the study area, utilizing cloud-based remote sensing and optimized mangrove vegetation indices within GEE; and (2) construct a physical accounting table. Thus, this study will contribute to the broader effort of establishing SEEA-compliant ecosystem accounts for the West Philippine Sea, providing critical data for evidence-based policymaking.

MATERIALS AND METHODS

Study Site

The research was conducted in the mangrove habitats of Occidental Mindoro, Philippines, in September 2023. The province is part of Region IV-B (MIMAROPA-Mindoro (Occidental Mindoro), Marinduque, Romblon, and Palawan), which is located in the southwest of the country and is bordered by the Sulu Sea and the West Philippine Sea (Figure 1). Occidental Mindoro has a total land area of 597,228.63 ha accounting for 2 percent of the Philippines' total land area (HDX 2016). The pilot site is part of the project "Natural Capital Accounting of Coastal and Marine Ecosystems in the West Philippine Sea," under the program "Resource Inventory, Valuation and Policy in Ecosystems Services Under Threat (RE-INVEST): The Case of West Philippine Sea," (RE-INVEST WPS Project 2) with project duration from April 2022 to March 2025. Implementation sites include Kalayaan Island Group, Western Palawan, Occidental Mindoro, Oriental Mindoro, Bataan, Zambales, and Pangasinan funded by the Department of Science and Technology - Philippine Council for Agriculture, Aquatic and Natural Resources Research and Development (DOST-PCAARRD). The methodology flowchart in mangrove ecosystem mapping using developed mangrove vegetation indices is illustrated in Figure 2.

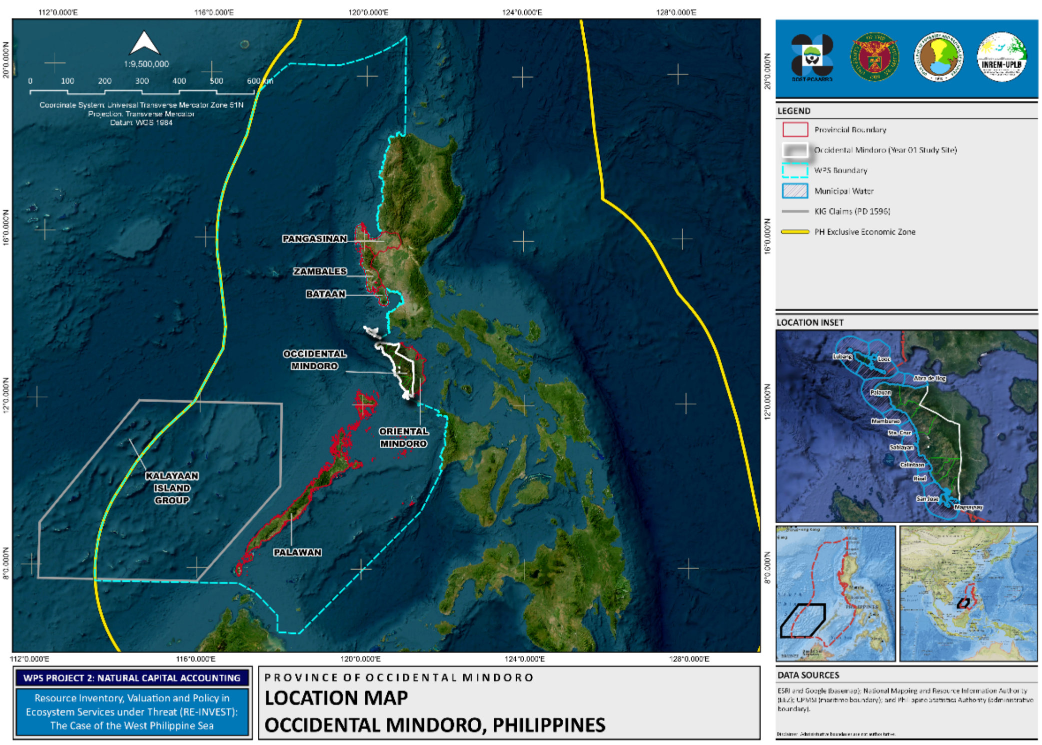

Figure 1: Location map of Occidental Mindoro, Philippines in the West Philippine Sea

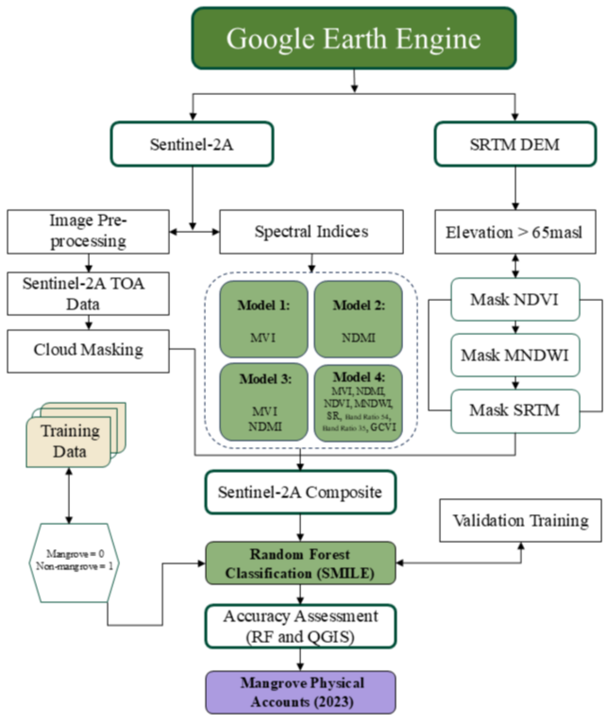

Figure 2: Methodology flowchart in mangrove ecosystem mapping using developed mangrove vegetation indices

Satellite Data and Pre-Processing

Sentinel-2 Multispectral Imager Instrument (MSI) Level-2A imagery of the Occidental Mindoro coastline was obtained from the Sentinel Scientific Data Hub (European Space Agency 2018). Top-of-Atmosphere (ToA) reflectance data previously has been orthorectified, georeferenced, and radiometrically calibrated.

The study site is set on the coastal areas of Occidental Mindoro, estimated at 1 km landward and 300 m seaward. The maskClouds function was employed to generate cloud-free mosaics from satellite imagery. It operates by identifying and masking cloud-contaminated pixels, effectively assigning them a null value. This process renders these pixels transparent during image compositing, thus excluding them from the region of interest and ensuring accurate analysis of the underlying surface (Google Earth Engine, no date). Next, is by adding the spectral indices designed for mangrove vegetation in a pixel, as well as water features (Table 1). This study evaluated four distinct models, each utilizing different combinations of spectral indices to assess mangrove characteristics. These models included: (1) the Mangrove Vegetation Index (MVI), (2) the Normalized Difference Mangrove Index (NDMI), (3) a combined MVI and NDMI Model, and (4) an expanded model incorporating MVI, NDMI, and additional spectral indices. The supplementary indices in the fourth model consisted of the Modified Normalized Difference Water Index (MNDWI), Green Chlorophyll Vegetation Index (GCVI), simple ratio, band ratio 5/4, and band ratio 3/5.

Table 1: Spectral indices for mangrove mapping using Sentinel-2A imagery

Spectral Indices	Band Ratio	Source
Mangrove Vegetation Index (MVI)		Baloloy et al. (2020)
Normalized Difference Mangrove Index (NDMI)		Shi et al. (2016)
Normalized Difference Vegetation Index (NDVI)		Kogan (1995) and Tarplet et al. (1984)
Modified Normalized Difference Water Index (MNDWI)		Xu (2006)
Green Chlorophyll Vegetation Index (GCVI)		Gitelson et al. (2003)
Simple Ratio (SR)		Birth and McVey (1968)
Ratio 54 (Difference between bands 5 and 4)		-
Ratio 35 (Difference between bands 3 and 5)		-

Furthermore, temporal parameters set within April 2021 to June 2023, the start and end months are characterized as the dry season in the Philippines, thus creating cloud-free images. Additionally, the study area is filtered with the Shuttle Radar Topography Mission (SRTM) Digital Elevation Model by filtering elevations less than 65 m above sea level with NDVI and MNDWI masks. Mangrove habitat delineation was refined through the application of masking procedures to NDVI, MNDWI, and digital elevation model (DEM) data. This process aimed to isolate areas characterized by high vegetation density, exclude water-influenced areas, and constrain the analysis to elevation ranges known to support mangrove ecosystems within the study region (Figure 3).

Figure 3: Composite images of the coastal areas of Sablayan, Occidental Mindoro, Philippines in the West Philippine Sea

Constructing the Random Forest Classification

The Random Forest (RF) machine learning method, introduced by Breiman (2001), employs an ensemble of decision trees for classification and prediction. Each tree contributes a single vote, and the result is determined by a majority voting process. Notably, RF exhibits advantages such as intuitive parameterization and robustness to collinear features and high-dimensional data (Pelletier et al., 2016).

In this study, the smileRandomForest classifier, part of the Statistical Machine Intelligence and Learning Engine (SMILE) library was utilized. Developed to enhance the performance and stability of earlier GEE classifiers, smileRandomForest is primarily designed for supervised classification. It operates by assigning data points, such as satellite image pixels, to predefined categorical classes based on input features. This is achieved through the construction and aggregation of individual decision tree predictions, a process that improves classification accuracy and reduces overfitting compared to single decision tree methods.

Furthermore, SMILE can be directly implemented within GEE to assess its features of importance. However, as demonstrated by Jastrzebski (2018), accurate quantification of feature importance in RF models using SMILE requires a balanced distribution of reference data. A map showing the distribution of mangrove areas (identified by mangrove pixels) in Santa Cruz, Occidental Mindoro is illustrated in Figure 4.

Figure 4: Estimated mangrove extent, derived from pixel classification, for the Municipality of Santa Cruz, Occidental Mindoro

Formulation of combined vegetation indices

This study utilized mangrove vegetation indices, including MVI, NDVI, NDMI, the Modified MNDWI, and GCVI. In contrast, these vegetation indices exhibited bands capable of reflecting the spectral waves in mangrove ecosystems. According to Baloloy et al. (2020), studies related to mangrove vegetation properties and spectral responses, short wave infrared 1 (SWIR1), Near-Infrared (NIR) (Band 8), and green (Band 3) are the three multispectral bands usually found in MVI. The utilization of SWIR and NIR bands has been determined to be highly effective in the characterizations of water absorption in vegetation and the assessment of vegetation greenness, respectively (Manna and Raychaudhuri, 2020; Wang et al., 2018).

Index Accuracy Assessment

To ensure a representative dataset for model training and validation, a stratified random sampling approach was employed utilizing GEE. A total of 300 sampling points were generated within the coastal areas of Occidental Mindoro. Stratification was implemented to proportionally represent both mangrove and non-mangrove classes, thereby minimizing bias and enhancing the reliability of subsequent analyses. This was achieved through the creation of a stratPoints FeatureCollection within GEE, where random points were generated and assigned class labels based on a pre-existing classification layer. The stratPoints collection ensured that the sampling points were spatially distributed across the defined coastal extent of Occidental Mindoro, effectively capturing the inherent variability of the study area. Stratified random sampling, implemented via GEE, yielded a strong and representative dataset, essential for the accurate training and validation of the Random Forest classification model.

For the Accuracy Assessment, the overall accuracy, user's accuracy and producer's accuracy, and kappa coefficient were assessed using the following formula:

Equation 1:

$$Overall\ Accuracy\ (OA) = \frac{\sum_{i=1}^{k} \quad n_{jj}}{N}$$

Where:
n_{ii} = number of correctly classified samples for class i (diagonal elements of the confusion
matrix)
k = total number of classes
N = total number of reference (ground truth) samples

Equation 2:

$$User's\ Accuracy\ (UA) = \frac{n_{ii}}{\sum_{j=1}^{k} \quad n_{ji}}$$

Where:
n_{ii} = correctly classified samples for class i
$\sum_{j=1}^{k} \quad n_{ji}$ = total number of samples classified as class i

Equation 3:

$$Producer's\ Accuracy\ (UA) = \frac{n_{ii}}{\sum_{j=1}^{k} \quad n_{ij}}$$

Where:
n_{ii} = correctly classified samples for class i
$\sum_{j=1}^{k} \quad n_{ij}$ = total number of actual (reference) samples for class i

Equation 4:

$$K = \frac{Po - Pe}{1 - Pe}$$

Where:
Po = overall accuracy of the model
Pe = measure of the agreement between the model predictions and the actual class values as if happening by chance

Overall, accuracy represents the percentage of the mapped area that aligns with the reference data, indicating the likelihood of a random point on the map being correctly categorized. User's accuracy quantifies the reliability of a specific class on the map, showing the probability that a location identified as class 'i' truly corresponds to class 'i' in the reference. Producer accuracy measures how well a specific reference class is represented on the map, reflecting the probability that a location of reference class 'j' is correctly classified as class 'j' in the map.

Development of Mangrove Physical Accounts

A three-tiered approach based on the System of Environmental Economic Accounting SEEA spatial framework for modeling was used to develop the mangrove extent. This study's limitations include its focus on estimating the recent mangrove extent and classifying land cover into binary categories of mangrove and non-mangrove. To expand the scope beyond mangrove/non-mangrove classification, future research can incorporate a comprehensive land and marine cover classification, utilizing the NAMRIA land cover dataset and coastal resources map, which includes mangroves as a distinct class. A consistent methodology can be applied to coastal and marine areas within the 2015 and 2020 datasets to construct opening and closing physical account tables for Occidental Mindoro. However, the optimal classification model developed in this study was employed to reclassify newly identified mangrove areas, facilitating the creation of updated mangrove physical accounts for subsequent analyses.

RESULTS AND DISCUSSION

Cloud Free Annual Mosaic of Sentinel-2A

Clouds and shadows were noted in the Sentinel-2A image series from 2021 to 2023 and are regarded as one of the challenges, particularly in the Philippines, when dealing with remotely sensed photos. The presence of various objects such as clouds, haze, and shadows, may have an impact on the model's overall performance in capturing changes in mangrove cover mapping, leading to inaccuracies, inconsistencies, and false detection making long-term mapping and monitoring of coastal ecosystems challenging (Mwita et al., 2012; Cihlar, 2000). To filter clouds, the study employed images with less than 20 percent cloud coverage. The median was used to consolidate the collection of photos, minimizing the image collection by computing the median of all values at each pixel across all matching bands.

Developed Mangrove Vegetation Indices and Random Forest Classification

The coastal mangrove vegetation in Occidental Mindoro, Philippines was evaluated using Sentinel-2A's spectral color composition and different combinations of developed indices produced by Shi et al. (2016) and Baloloy et al. (2020). Before using smileRandomForest to classify mangroves, variables such as elevation data (<65 m above sea level) and composite images were used to differentiate between mangroves and non-mangroves. Setting the parameters for mangrove filtering enabled the removal of areas in elevations above 65 masl. The adjustment was determined by the absolute difference between ICESat-2 ground elevation data and the TanDEM-X DEM. This approach resulted in a discrepancy of less than 50 meters, a threshold applied in Yu et al.'s (2024) global mangrove canopy height mapping study.

To assess the performance of different RF classification results, the total pixel sample and number of training and testing data were examined, with 80 percent used for training data and the remaining 20 percent for testing data. Machine learning models were validated by dividing data into training and testing sets, where the training set, with labeled data, was used for model development (Salazar et al., 2022). The separation of data into training and testing sets was a critical step in the machine learning workflow. This allows the model to learn through the discovery of patterns and relationships within the dataset (Sivakumar, 2024). As a general rule, the training set is larger than the testing set, and in this study, it was set at 80 percent. This decision was based on the understanding that a larger training set typically results in improved model performance. Testing, on the other hand, was used to evaluate the model's performance, including its ability to avoid overfitting and underfitting.

The mangrove and non-mangrove covers were assigned values of 1 and 0, respectively. Each scenario, which comprised both a stand-alone index and a combination of recognized mangrove vegetation indices, was tested to evaluate how they performed when mapping mangrove areas. The Mangrove Vegetation Index or Model 1 (MVI) and the Normalized Difference Mangrove Index or Model 2 (NDMI) have similar total sample pixel sizes (253,234 and 253,227, respectively), as well as mangrove extents (2,124.41 and 2,161.64 hectares). However, there are minor differences in the number of training and testing data. MVI has 202,686 training data pixels, but NDMI has 202,616, indicating that MVI used 70 more training data pixels than NDMI during classification. On the other hand, MVI has 50,548 tested data pixels, whereas NDMI has 50,611, indicating that NDMI has 63 more tested data pixels than MVI.

The study encompassed the combination of vegetation indices, including MVI and NDMI (Model 3), and a combination of MVI and NDMI, as well as MVI and NMDI and other spectral indices referred to as Model 4. Both vegetation indices captured a comparable number of mangroves, with combined MVI and NDMI and other spectral indices (Model 4) resulting in a mangrove extent of 2,096.74 ha and combined MVI and NDMI (Model 3) resulting in 2,085.41 ha. Both Models 3 and 4 employed a comparable total sample pixel count of 253,219 and 253,226 pixels, respectively. Figure 5 presents a comparison of mangrove distribution maps generated by four different modeling approaches.

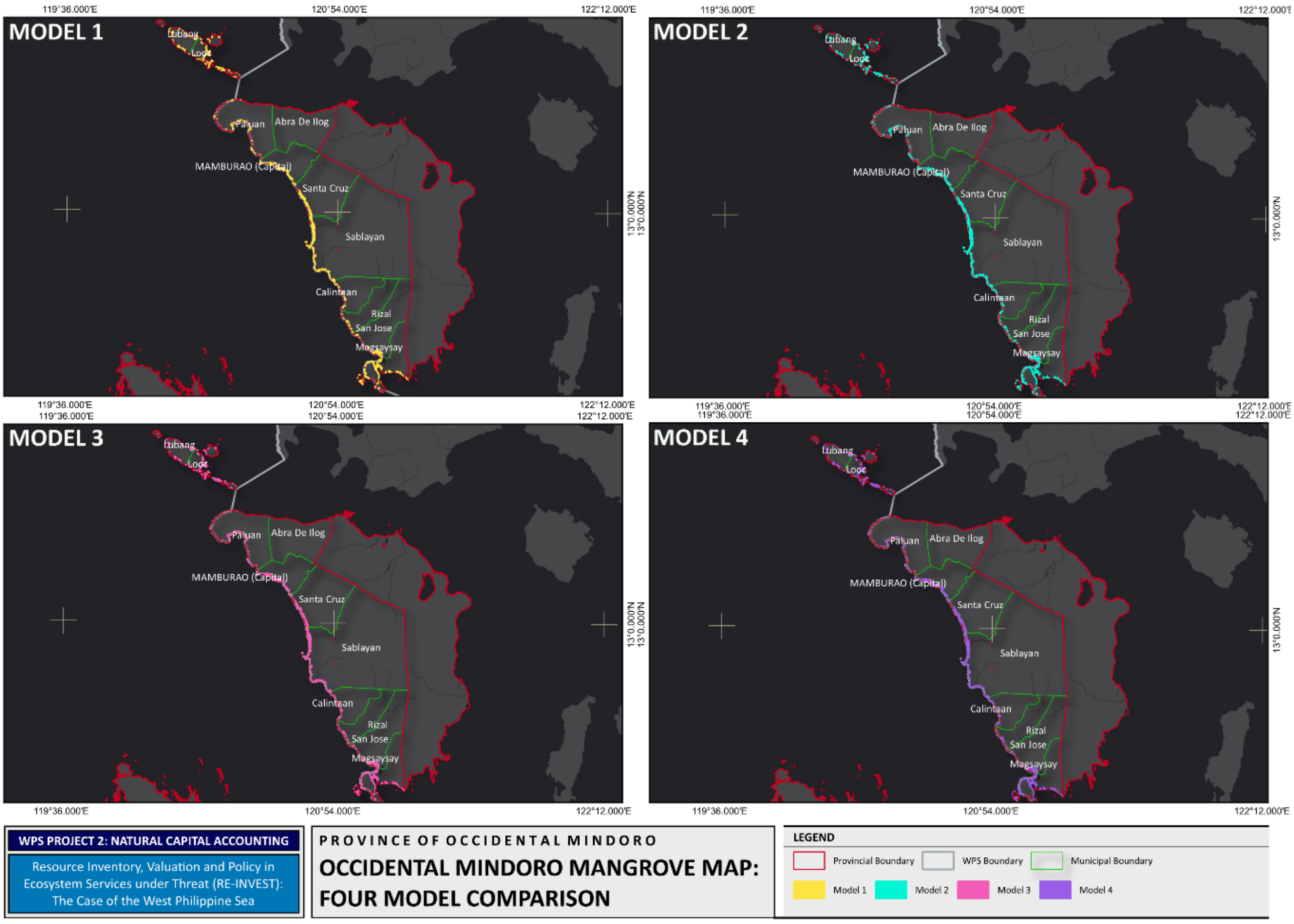

Figure 5: Comparison of Four models of Occidental Mindoro mangrove map

Models 3 and 4 utilized marginally different training and testing datasets. Specifically, Model 4, incorporating combined MVI, NDMI, and additional spectral indices, employed 202,597 training pixels, while Model 3, using only combined MVI and NDMI, utilized 202,856 pixels. Similarly, Model 4 used 50,629 testing pixels, compared to 50,363 in Model 3. These minor variations in training and testing dataset sizes, observed across all models, are attributed to the consistent image data and the fixed train-test split ratio employed throughout the study. Notably, a larger training dataset is known to improve model learning capabilities (Sivakumar, 2024). All models were designed with an equivalent number of classes in both training and testing datasets to achieve class balance. This strategic approach was adopted to minimize bias during the training-testing split and to ensure a robust and equitable evaluation of model performance, thus providing stable results, which are essential for reliable model comparisons (Sivakumar, 2024). The summary of the number of sample pixels on training and testing data, and the total extent of mangroves in Occidental Mindoro, Philippines, is illustrated in Table 2.

Table 2: Number of sample pixels on training and testing data, and total extent of mangroves in Occidental Mindoro, Philippines

Vegetation Indices for Mangroves	Total Sample Pixel	Number Training Data (Pixels)	Number of Tested Data (Pixels)	Extent of Mangroves (ha)
Mangrove Vegetation Index	253,234	202,686	50,548	2,124.41
Normalized Difference Mangrove Index	253,227	202,616	50,611	2,161.64
Combined MVI and NDMI	253,219	202,856	50,363	2,085.41
Combined MVI and NDMI and other Spectral Indices	253,226	202,597	50,629	2,096.74

Mangrove Extent Coverage and Accuracy Assessment

Accuracy was assessed using key performance metrics, specifically overall accuracy, user's accuracy, producer's accuracy, and the Kappa coefficient. The combined spectral indices (Model 4) had the highest overall accuracy (87.33%), followed by NDMI or Model 2 (85.67%), MVI (Model 1) (83.33%), and the combined MVI and NDVI Model (Model 3) (82.33%).

User's accuracy determines if a pixel labeled as mangrove truly represents one. The combination of MVI and NDMI had the lowest user's accuracy (65.63%), followed by the MVI method (67.97%) and NDMI (72.66%), while the combination of all spectral indices (Model 4) produced the best user's accuracy in mangroves (76.19%). An actual mangrove pixel is likely to be classified as such based on producer's accuracy. The NDMI has the highest producer's accuracy (92.08%), followed by the MM (90.63%), the combination of all spectral indices (90.48%), and the NDMI. The Kappa coefficient provides a quantitative measure of agreement between observed and predicted categorical classifications, accounting for the possibility of agreement occurring by chance. A high Kappa coefficient indicates a strong concordance between the classified image generated by the model and the reference data. Comparative analysis of kappa coefficients demonstrated that Model 4 (0.80), utilizing a combination of MVI, NDMI, and other spectral indices, outperformed the other models. Specifically, NDMI (Model 2) achieved a kappa of 0.75, combined MVI and NDMI (Model 3) resulted in 0.70, and MVI (Model 1) yielded 0.65.

Among all models, Model 4 or the combination of all eight spectral indices resulted in an overall mangrove extent of about 2,096.74 ha, with a classification accuracy of 87.33 percent and a Kappa coefficient of 0.80 using 300 stratified random points generated in GEE (Table 3). Compared to employing MVI and NDMI independently, the combined spectral indices (Model 4) demonstrated the highest accuracy among the four RF scenarios. However, the independent accuracies of NDMI and MVI resulted in a closer overall accuracy of 85.67 percent and 83.33 percent, respectively.

Table 3: Mangrove class accuracy (user accuracy (UA) and producer accuracy (PA) and overall accuracy (OA) and Kappa Statistic (K) calculated from Random Forest Classification

Vegetation Indices for Mangroves	Overall Accuracy (%)	User Accuracy (%)		Producer Accuracy (%)		Kappa Coefficient
		Mangroves	Non-Mangroves	Mangroves	Non-Mangroves	
Mangrove Vegetation Index	83.33	67.97	94.77	90.63	79.9	0.65
Normalized Difference Mangrove Index	85.67	72.66	95.35	92.08	82.41	0.70
Combined MVI and NDMI	82.33	65.63	94.77	90.32	78.74	0.70
Combined MVI and NDMI and other Spectral Indices	87.33	76.19	95.98	90.48	84.34	0.80

The validation error matrix for the Random Forest classification using Model 4 revealed a detailed picture of the model's performance in distinguishing between mangrove and non-mangrove areas. The matrix indicated 28,689 pixels correctly classified as non-mangrove (True Negatives), while 19,102 pixels were accurately identified as mangrove (True Positives). However, the model also exhibited errors: 1,052 non-mangrove pixels were misclassified as mangrove (False Positives or commission errors), and 1,786 mangrove pixels were incorrectly labeled as non-mangrove (False Negatives or omission errors). Based on these values, the overall accuracy of the model was calculated to be approximately 94.6 percent, demonstrating a high degree of correctness in the classification. Further analysis revealed a precision of approximately 94.8 percent for mangrove classification, indicating that when the model predicted mangrove, it was correct nearly 95 percent of the time. The recall, or sensitivity, which measures the model's ability to identify all actual mangrove areas, was approximately 91.5 percent. These metrices collectively illustrate robust model performance, though with identifiable commission and omission errors, which should be considered in the interpretation of the resulting mangrove map.

Mangrove Ecosystem for Coastal and Marine Ecosystem Physical Accounting

The development of a delineated ecosystem supplies information on its extent, condition, monetary values, and its capacity to provide ecosystem services. These assets reflect a distinct boundary between biotic and abiotic components and their interactions. Moreover, these ecosystems are presented in the form of a physical map or table that displays their location, areal components, and spatial characteristics. For this study, the System of Environmental-Economic Accounting for Ecosystem Accounting illustrated that the most practical way to present a delineated ecosystem is by providing a measure of the surface area for different ecosystem types (United Nations, 2022).

A limitation of this study is the absence of a comprehensive analysis of opening and closing extents for coastal and marine ecosystems within the province. To address this, Model 4 was used to integrate the derived mangrove extent with the most recent National Mapping and Resource Information Authority mangrove dataset. This integration, in comparison to the 2015 NAMRIA dataset, facilitated the development of a physical extent account for the province. The 2015 marine and land cover maps produced by NAMRIA were derived from a digital/visual classification of 30-meter resolution Landsat 8 satellite imagery, supplemented by other available high-resolution satellite data, utilizing remote sensing and GIS techniques. In contrast, the 2020 dataset was generated through digital interpretation of 10-meter resolution Sentinel 2 imagery from the European Space Agency (ESA), spanning the period 2017-2021, and incorporating additional high-resolution satellite imagery.

Table 4: Ecosystem type change matrix for Occidental Mindoro's coastal and marine ecosystems (2015-2023)

		Mangrove Forest	Corals	Seagrass/ Seaweeds	Open Water	Annual Crop	Brush/ Shrubs	Built-up	Fishpond	Grassland	Inland Water	Open Forest	Open/ Barren	Perennial Crop	Total	
Opening Extent 2015		**1,277.45**	**5,057.55**	**17,868.09**	**692,121.98**	**2,173.04**	**17,320.24**	**11,205.23**	**2,873.41**	**2,087.18**	**3,001.82**	**3,745.49**	**1,013.59**	**1,156.90**	**760,901.97**	
Addition																
Addition from:	Mangrove Forest		6.91	0.02	44.45	-	155.93	187.03	52.29	12.43	42.52	208.63	90.84	38.26	839.30	Total Reduction from Mangrove Forest
	Corals	3.40		308.86	750.73	0.39	20.46	8.90	12.28	1.58	7.68	10.65	5.89	23.12	1,153.94	Total Reduction from Corals
	Seagrass/Seaweeds	-	316.69		2,841.57	0.88	6.04	0.36	0.52	0.55	0.37	-	-	2.95	3,169.93	Total Reduction from Seagrass/Seaweeds
	Open Water	4.55	518.05	3,883.20		4.11	148.92	29.09	35.91	13.25	52.11	16.19	18.08	241.38	4,964.83	Total Reduction from Open Water
	Annual Crop	-	0.47	0.00	22.47		304.30	10.44	5.54	23.39	-	0.20	10.69	10.45	387.96	Total Reduction from Annual Crop
	Brush/Shrubs	21.45	18.72	1.39	107.45	271.32		1,065.25	488.81	402.40	103.29	43.68	48.05	95.12	2,666.93	Total Reduction from Brush/Shrubs
	Built-up	21.47	3.17	0.41	25.29	5.12	524.58		480.24	53.19	342.53	81.05	86.26	94.53	1,717.82	Total Reduction from Built-up
	Fishpond	1.78	2.24	2.41	18.25	2.14	175.53	390.44		14.36	143.10	20.51	19.56	22.57	812.90	Total Reduction from Fishpond
	Grassland	1.31	0.69	1.83	34.85	58.67	1,042.39	118.88	28.91		23.50	2.98	58.88	72.21	1,445.09	Total Reduction from Grassland
	Inland Water	4.85	4.77	0.57	13.97	-	93.91	362.66	84.76	13.34		30.04	17.93	35.31	662.10	Total Reduction from Inland Water
	Open Forest	16.06	1.25	-	10.03	2.79	35.76	108.25	38.89	2.80	16.67		47.58	16.87	296.95	Total Reduction from Open Forest
	Open/Barren	8.36	6.66	-	41.47	2.64	28.76	88.33	22.60	9.58	28.04	47.79		52.28	336.51	Total Reduction from Open/Barren
	Perennial Crop	6.59	28.57	1.75	154.60	5.53	90.63	79.10	71.70	31.79	70.09	3.44	76.96		620.76	Total Reduction from Perennial Crop
	Total addition	**89.82**	**908.20**	**4,200.43**	**4,065.12**	**353.59**	**2,627.23**	**2,448.73**	**1,322.43**	**578.66**	**829.88**	**465.18**	**480.72**	**705.06**	**19,075.03**	
Reduction																
Converted to:	Mangrove Forest		3.40	-	4.55	-	21.45	21.47	1.78	1.31	4.85	16.06	8.36	6.59	89.82	Total Addition to Mangrove Forest
	Corals	6.91		316.69	518.05	0.47	18.72	3.17	2.24	0.69	4.77	1.25	6.66	28.57	908.20	Total Addition to Corals
	Seagrass/Seaweeds	0.02	308.86		3,883.20	0.00	1.39	0.41	2.41	1.83	0.57	-	-	1.75	4,200.43	Total Addition to Seagrass/Seaweeds
	Open Water	44.45	750.73	2,841.57		22.47	107.45	25.29	18.25	34.85	13.97	10.03	41.47	154.60	4,065.12	Total Addition to Open Water
	Annual Crop	-	0.39	0.88	4.11		271.32	5.12	2.14	58.67	-	2.79	2.64	5.53	353.59	Total Addition to Annual Crop
	Brush/Shrubs	155.93	20.46	6.04	148.92	304.30		524.58	175.53	1,042.39	93.91	35.76	28.76	90.63	2,627.23	Total Addition to Brush/Shrubs
	Built-up	187.03	8.90	0.36	29.09	10.44	1,065.25		390.44	118.88	362.66	108.25	88.33	79.10	2,448.73	Total Addition to Built-up
	Fishpond	52.29	12.28	0.52	35.91	5.54	488.81	480.24		28.91	84.76	38.89	22.60	71.70	1,322.43	Total Addition to Fishpond
	Grassland	12.43	1.58	0.55	13.25	23.39	402.40	53.19	14.36		13.34	2.80	9.58	31.79	578.66	Total Addition to Grassland
	Inland Water	42.52	7.68	0.37	52.11	-	103.29	342.53	143.10	23.50		16.67	28.04	70.09	829.88	Total Addition to Inland Water
	Open Forest	208.63	10.65	-	16.19	0.20	43.68	81.05	20.51	2.98	30.04		47.79	3.44	465.18	Total Addition to Open Forest
	Open/Barren	90.84	5.89	-	18.08	10.69	48.05	86.26	19.56	58.88	17.93	47.58		76.96	480.72	Total Addition to Open/Barren
	Perennial Crop	38.26	23.12	2.95	241.38	10.45	95.12	94.53	22.57	72.21	35.31	16.87	52.28		705.06	Total Addition to Perennial Crop
	Total Reduction	**839.30**	**1,153.94**	**3,169.93**	**4,964.83**	**387.96**	**2,666.93**	**1,717.82**	**812.90**	**1,445.09**	**662.10**	**296.95**	**336.51**	**620.76**	**19,075.03**	
Closing Extent 2020 (2023 for mangrov		**2,026.94**	**5,303.29**	**16,837.59**	**693,021.69**	**2,207.41**	**17,359.95**	**10,474.32**	**2,363.88**	**2,953.62**	**2,834.04**	**3,577.26**	**869.39**	**1,072.60**	**760,901.97**	
Net Change in Extent		**(749.49)**	**(245.74)**	**1,030.50**	**(899.71)**	**(34.37)**	**(39.70)**	**730.91**	**509.53**	**(866.43)**	**167.78**	**168.23**	**144.21**	**84.30**	**-**	
Extent Retained		**1,187.64**	**4,149.35**	**13,667.65**	**688,056.86**	**1,819.45**	**14,693.02**	**8,756.50**	**1,550.98**	**1,508.53**	**2,171.94**	**3,280.31**	**532.88**	**451.84**	**741,826.94**	

In terms of mangrove ecosystems, datasets on land cover and coastal resources maps are significant information as they provide knowledge on the amount and type of vegetation present from ridges up to the reef. Vegetation types affect the goods and services that an ecosystem can provide. Recalculation was done using Model 4, as post-processing was implemented in the mangrove extent. Discrepancies in areal measurements were observed due to methodological differences in defining the region of interest. Specifically, the region of interest employed in Google Earth Engine differed from the precise extent processed in Quantum Geographic Information System (QGIS 3.34.5-Prizren), which was reprojected to World Geodetic System (WGS 1984 Zone 51 North), a coordinate system geographically optimized for Mindoro Island.

Based on NAMRIA's overlaid data and developed mangrove extent, it recorded an area of 1,277.45 ha in 2015 and 2,026.94 hectares by 2023 (Table 8). Over the nine years from 2015 to 2023, a net gain of 749.49 ha (58.67%) in mangrove area extent was observed. While Lubang (6.59 ha, 41.87% relative change), Rizal (9.69 ha, 58.47%), Calintaan (13.75 ha, 54.51%), and Looc (17.05 ha, 17.71%) experience the least increase in mangrove extent, the remaining municipalities exhibited an increase ranging from 40 to 325 ha. Notably, Sablayan (324.90 ha, 163.89%), San Jose (170.24 ha, 54.84%), and Magsaysay (117.61 ha, 81.35%) showed the most substantial expansion. With the extent retained in mangrove ecosystem of 1,187.64 ha, the primary drivers of mangrove increase were conversion from brush/shrubs (21.45 ha), agricultural areas (23.25 ha), aquaculture (16.06 ha), and inland water bodies (8.36 ha). Additionally, an increase in mangrove extent was also observed within water bodies (4.55 ha) and seagrass/seaweed beds (3.40 ha).

CONCLUSION

This study utilized the use of Google Earth Engine (GEE) and Sentinel 2-A satellite images using the Random Forest Classification algorithm and mangrove indices to develop the extent of mangroves. GEE offers substantial computational capabilities and an extensive collection of remote sensing data and supplemental datasets, which collectively enhance the development of precise mapping accuracy. Additionally, random forests were excellent for assessing the physical accounts of mangroves while also detecting vegetation in a quick, consistent, and precise manner. Sentinel-2A and the GEE were useful tools for monitoring and assessing coastal and marine ecosystems. Furthermore, the best mangrove discrimination in the RF classifier was achieved when the combination of various developed mangrove vegetation indices and spectral indices was used, Model 4 of the study. The overall accuracy achieved by the RF classifier was 87.33 percent and 0.80 for the Kappa coefficient. Meanwhile, MVI and NDMI overall accuracy accounted for 83.33 percent and 85.67 percent, and Kappa coefficients of 0.64 and 0.70, respectively. Additionally, Model 4, a Random Forest classification, achieved 94.6 percent overall accuracy in distinguishing mangrove and non-mangrove areas, with 28,689 true negatives and 19,102 true positives. However, the model showed 1,052 commission errors and 1,786 omission errors, resulting in 94.8 percent precision and 91.5 percent recall. While demonstrating robust performance, these errors should be considered when interpreting the final mangrove map. Hence, Model 4, employing a combination of vegetation indices and proper band selection for mangroves, enhances mapping extent quality while increasing spectral information through providing a richer spectral signature, which can improve the model's ability to distinguish between land cover types. Consequently, the accuracy metrics of the other models demonstrated promising results, indicating their suitability for mangrove extent mapping. These findings suggest that multiple model approaches can yield reliable estimates of mangrove extent and further develop independent assessment and inter-comparison of mangrove maps using both national and global datasets.

ACKNOWLEDGEMENT

This study was funded by the Department of Science and Technology's Philippine Council for Agriculture, Aquatic, and Natural Resources Research and Development. The University of the Philippines Los Baños Interdisciplinary Studies Center for Integrated Natural Resource and Environment Management (UPLB-INREM) conducted this research.

CONFLICT OF INTEREST

The authors declare that there is no conflict of interest.

CONTRIBUTIONS OF INDIVIDUAL AUTHORS

Adrian Pablo V. Sasi (APVS) led the overall development and implementation of the study. He was supported by Dr. Cristino L. Tiburan Jr. (CLTJr) and Dr. Arnan B. Araza (ABA), who provided expertise in remote sensing and Geographic Information Systems. Dr. Gem B. Castillo (GBC) contributed to ecosystem accounting, while Dr. Canesio D. Predo (CDP) and Dr. Asa Jose U. Sajise (AJUS) provided economic insights. Dr. Rosario V. Tatlonghari (RVT), Dr. Catherine S. Anders (CSA), and Dr. Juan M. Puilhin (JMP) assisted with the analysis, editing, and proofreading of the manuscript.

For data gathering, the following authors conducted the necessary activities: APVS, CLTJr, GBC, CDP, AJUS, RVT, CSA, JMP, Christian Ray C. Buendia (CRCB), Dannica Rose G. Aquino (DRGA), Grace Anne S. Malolos (GASM), Karen M. Pajadan (KMP), and Pauline Cielo P. Palma (PCPP). All authors also contributed to the data analysis and manuscript writing.

REFERENCES

Addabbo P, et al. Contribution of Sentinel-2 data for applications in vegetation monitoring, Acta Imeko 2016; 5 (2):44.

Baloloy AB, Blanco AC, Sta. Ana RRC, Nadaoka K. Development and application of a new mangrove vegetation index (MVI) for rapid and accurate mangrove mapping. ISPRS J Photogramm Remote Sens 2020; 166:95-117.

Baloloy AB, et al. Development of a rapid mangrove zonation mapping workflow using Sentinel 2-derived indices and biophysical dataset. Front Remote Sens 2021; 2:730238.

Birth GS, McVey GR. Measuring the color of growing turf with a reflectance spectrophotometer 1. Agron J 1968; 60 (6):640–643.

Breiman L. Random forests. Mach Learn 2001; 45 (1):5-32.

Brown W, Fischer AF. Philippine mangrove swamps. Bureau of Printing, 1918.

Brown CF, et al. Dynamic world, near real-time global 10m land use land cover mapping. Scientific Data 9 2022. doi:10.1038/s41597-022-01307-4.

Carpenter KE, Springer VG. The center of the center of marine shore fish biodiversity: the Philippine Islands. Environ Biol Fish 2005; 72 (4):467–80.

Chrysafis I, et al. Retrieval of Leaf Area Index Using Sentinel-2 Imagery in a Mixed Mediterranean Forest Area. Int J Geo-Information 2020. 9 (11):622

Cihlar J. Land cover mapping of large areas from satellites: status and research priorities. Int J Remote Sens 2000; 21 (6–7):1093–114.

CIA. The World Factbook -- Field Listing - Coastline. 2007 Jun 13. Available from: https://web.archive.org/web/20070613004524/https://www.cia.gov/library/publications/the-world-factbook/fields/2060.htm

Deilmai BR, et al. Comparison of two classification methods (MLC and SVM) to extract land use and land cover in Johor, Malaysia. IOP Conf Ser Earth Environ Sci 2014; 20:012052.

Department of Environment and Natural Resources. Sustaining our coasts: the ridge-to-reef approach -- a compilation of technical and policy papers: mangrove management. Quezon City, Philippines: Integrated Coastal Resources Management Project, Department of Environment and Natural Resources, 2013: 79

Defourny P, et al. Land cover cci. Product User Guide Version 2 2012: 325.

Drusch M, et al. Sentinel-2: ESA's optical high-resolution mission for GMES operational services. Remote Sens Environ 2012; 120:25–36.

Eklundh L, Sjöström M, Ardö L, Jönsson P. High resolution mapping of vegetation dynamics from Sentinel-2. In: Proceedings of the First Sentinel-2 Preparatory Symposium; 2012; Frascati, Italy.

ESA Climate Change Initiative. Global Land Cover Maps, Version 2.0. 2017: Available from: https://maps.elie.ucl.ac.be/CCI/viewer. Accessed 2025 Mar

European Space Agency. The Copernicus Open Access Hub. Available from: https://dataspace.copernicus.eu/. Accessed 2023 Sep

Forest Management Bureau (FMB). Philippine forestry statistics: forest cover within forest lands: 2003. Quezon City: Forest Management Bureau, Department of Environment and Natural Resources, Quezon City

Garcia KB, Malabrigo PL, Gevaña DT. Philippines' mangrove ecosystem: status, threats and conservation. In: Faridah-Hanum I et al., eds. Mangrove Ecosystems of Asia: status, challenges and management strategies. Springer; 2014:81–94.

Gitelson A, Gritz, Y, Merzlyak M. Relationships between leaf chlorophyll content and spectral reflectance and algorithms for non-destructive chlorophyll assessment in higher plant leaves. J Plant Physiol 2003: 160(3):271–282.

Giri C, Muhlhausen J. Mangrove Forest distributions and dynamics in Madagascar (1975–2005). Sensors 2008; 8(4):2104–2117.

Giri C, et al. Status and distribution of mangrove forests of the world using earth observation satellite data. Global Ecology and Biogeography 2011: 154–159.

Google for Developers. Compositing, masking, and mosaicking | Google Earth Engine. Available from: https://developers.google.com/earth-engine/tutorials/tutorial_api_05. Accessed 2025 Mar 3.

Gorelick N, Hancher M, Dixon M, Ilyushchenko S, Thau D, Moore R. Google Earth Engine: planetary-scale geospatial analysis for everyone. Remote Sens Environ 2017: 202:18–27.

Humanitarian Data Exchange. 2016. Philippine Administrative Boundary. Humanitarian Data Exchange. https://data.humdata.org/dataset/cod-ab-phl

Immitzer M, et al. First experience with Sentinel-2 data for crop and tree species classifications in Central Europe. Remote Sens 2016; 8(3):166.

Jastrzębski S, et al. Learning to SMILE(S). 2016. Available from: https://doi.org/10.48550/ARXIV.1602.06289.

Jia M., et al. Mapping global distribution of mangrove forests at 10-m resolution. Science Bulletin 68 2023: 1306–1316.

Kanniah K, et al. Satellite images for monitoring mangrove cover changes in a fast growing economic region in southern Peninsular Malaysia. Remote Sens 2015: 7(11):14360–85.

Karra K, et al. Global land use/land cover with sentinel 2 and deep learning. IEEE international geoscience and remote sensing symposium IGARSS, IEEE 2021: 4704–4707.

Kogan FN. Droughts of the late 1980s in the United States as derived from NOAA polar-orbiting satellite data. Bull American Meteorol Soc 1995; 76(5):655–668.

Lasco RD, Veridiano RKA, Habito M, Pulhin FB. Reducing emissions from deforestation and forest degradation plus (REDD+) in the Philippines: will it make a difference in financing forest development? Mitig Adapt Strateg Glob Change 2013; 18(8):1109–1124.

Li B, et al. An improved global land cover mapping in 2015 with 30m resolution (glc-2015) based on a multisource product-fusion approach. Earth System Science Data 15 2023: 2347–2373. doi:10.5194/essd-15-2347-2023

Liu X, et al. Large-scale high-resolution coastal mangrove forests mapping across West Africa with machine learning ensemble and satellite big data. Front Earth Sci 2021; 8:560933.

Long JB, Giri C. Mapping the Philippines' mangrove forests using Landsat imagery. Sensors 2011; 11(3):2972–81.

Ma L, et al. A review of supervised object-based land-cover image classification." ISPRS J Photogramme Remote Sens 2017: 130:277–293.

Manna S, Raychaudhuri B. Mapping distribution of Sundarban mangroves using Sentinel-2 data and new spectral metric for detecting their health condition. Geocarto Int 2020; 35(4): 434–452.

Mariano H, et al. Abandoned fishpond reversal to mangrove forest: will the carbon storage potential match the natural stand 30 years after reforestation? Forests 2022; 13(6):847.

Mwita E, et al. Detection of small wetlands with multi sensor data in East Africa. Adv Remote Sens 2012; 1(3): 64–73.

National Mapping and Resource Information Authority. Land cover of the Philippines. 2020. https://geoportal.gov.ph/

Pelletier C, Valero S, Inglada J, Champion N, Dedieu G. Assessing the robustness of random forests to map land cover with high resolution satellite image time series over large areas. Remote Sens Environ 2016; 187:156–168.

Pillodar F, et al. Mangrove resource mapping using remote sensing in the Philippines: a systematic review and meta-analysis. Forests 2023; 14(6):1080.

Primavera Ju, Sadaba R, Lebata J, Altamirano J. Handbook of mangroves in the Philippines, Panay. Southeast Asian Fisheries Development Center, Aquaculture Dept.: UNESCO Man and the Biosphere, 2004.

Rao M, et al. Mapping drought-impacted vegetation stress in California using remote Sensing. GISciRemote Sens 2017; 54(2):185–201.

Roslani MA, et al. Classification of mangroves vegetation species using texture analysis on Rapideye satellite imagery. 2003; 480–486.

Salazar JJ, et al. Fair train-test split in machine learning: mitigating spatial autocorrelation for improved prediction accuracy. J Pet Sci and Eng 2022; 209:109885.

Shi T, et al. New spectral metrics for mangrove forest identification. Remote Senss Letters 2016; 7(9):885–894

Simard M, et al. Global mangrove distribution, aboveground biomass, and canopy height. ORNL DAAC 2019.

Sivakumar M, et al. Trade-off between training and testing ratio in machine learning for medical image processing. PeerJ Comput Sci 2024; 10 :e2245.

Tarpley JD, Schneider SR, Money RL. Global vegetation indices from the NOAA-7 meteorological satellite. J Clim and Appl Meteorol 1984; 23(3):491–494.

Tomppo E, et al. Combining national forest inventory field plots and remote sensing data for forest databases. Remote Sens Environ 2008; 112 (5)1982–1999.

Topaloğlu RH, et al. Assessment of classification accuracies of Sentinel-2 and Landsat-8 data for land cover/use mapping. Int Arch Photogramm Remote Senss Spatial Inf Sci 2017; XLI-B8:1055–1059.

United Nations, European Commission, Food and Agriculture Organization, International Monetary Fund, Organisation for Economic Co-operation and Development, and World Bank. System of Environmental-Economic Accounting—Ecosystem Accounting (SEEA EA). White cover publication, pre-edited text subject to official editing. 2021. Available from: https://seea.un.org/ecosystem-accounting

United Nations. Guidelines on biophysical modelling for ecosystem accounting. New York: United Nations Department of Economic and Social Affairs, Statistics Division; 2022

Winarso G, et al. Comparison of mangrove index (MI) and normalized difference vegetation index (NDVI) for the detection of degraded mangroves in Alas Purwo Banyuwangi and Segara Anakan Cilacap, Indonesia. Ecol Eng 2023; 197:107119.

Xu H. Modification of normalised difference water index (NDWI) to enhance open water features in remotely sensed imagery. Int J Remote Sens 2006; 27(14):3025–3033.

Yu J, et al. Mapping global mangrove canopy height by integrating Ice, Cloud, and Land Elevation Satellite-2 photon-counting LiDAR data with multi-source images." Sci Total Environ 2024; 939:173487.

Zhu Z, Woodcock CE. Object-based cloud and cloud shadow detection in Landsat imagery. Remote Sens Environ 2012; 118:83–94.